Effect of radio-frequency bias voltage on the optical and structural properties of hydrogenated amorphous silicon carbide

J. Cui, Rusli,[a] and S. F. Yoon
School of Electrical and Electronic Engineering, Nanyang Technological University, Nanyang Avenue, Singapore 639798, Republic of Singapore

E. J. Teo
Department of Physics, Research Centre for Nuclear Microscope, National University of Singapore, 10 Kent Ridge Crescent, 119260 Singapore

M. B. Yu, K. Chew, J. Ahn, and Q. Zhang
School of Electrical and Electronic Engineering, Nanyang Technological University, Nanyang Avenue, Singapore 639798, Republic of Singapore

T. Osipowicz and F. Watt
Department of Physics, Research Centre for Nuclear Microscope, National University of Singapore, 10 Kent Ridge Crescent, 119260 Singapore

(Received 17 November 2000; accepted for publication 1 March 2001)

Hydrogenated amorphous silicon carbide (a-$Si_{1-x}C_x$:H) films have been deposited using the electron cyclotron resonance chemical vapor deposition process under varying negative rf-bias voltage at the substrate. The optical and structural properties of these films are characterized using Rutherford backscattering spectroscopy, transmittance/reflectance spectrophotometry, photothermal deflection spectroscopy, Fourier transform infrared absorption, Raman scattering, and room temperature photoluminescence (PL). These films deposited using a gas mixture of silane, methane, and hydrogen at a constant gas flow ratio showed a slight increase in the carbon fraction x, but very obvious structural transformation, at increasing rf induced bias voltage from -20 to -120 V. Near stoichiometric a-$Si_{1-x}C_x$:H films with a carbon fraction x of almost 0.5 are achieved at low bias voltage range from -20 to -60 V. Visible PL with relatively low efficiency can be observed from such films at room temperature. For larger bias voltages from -80 to -120 V, slightly C-rich a-$Si_{1-x}C_x$:H films ($x>0.5$) with larger optical gaps are obtained. These films have relatively higher PL efficiency, and the relative quantum efficiency was also found to depend strongly on the optical gap. Structurally, it was found that there is an increase in the hydrogen content and carbon sp^2 bonding in the films at larger bias voltages. The latter leads to an increase in the disorder in the films. The linear relationship observed between the Urbach energy E_0 and B factor in the Tauc equation suggests that the local defects related to microstructural disorder resulting from alloying with carbon dominate the overall defect structure of the films. Substrate biasing is noted to be crucial for the formation of Si–C bonds, as deduced from the Raman scattering results. *© 2001 American Institute of Physics.* [DOI: 10.1063/1.1367398]

I. INTRODUCTION

Hydrogenated amorphous silicon carbide (a-$Si_{1-x}C_x$:H) is an interesting material with various applications in solar cells, photoreceptors, and light-emitting diodes (LEDs).[1] As the band gap of a-$Si_{1-x}C_x$:H can be controlled by simply varying the carbon fraction, it is very suitable as a material for multicolor visible LEDs. Nontheless, a-$Si_{1-x}C_x$:H alloy remains a rather complex system to characterize due to the variety of bondings and disorders involved. Besides topological and compositional disorders, an additional source of variability derives from the ability of carbon to form sp^3, sp^2, and even sp^1 hybridization. As a result, the properties of a-$Si_{1-x}C_x$:H are highly dependent on the choice of deposition technique and conditions. Apart from the conventionally used rf plasma enhanced chemical vapor deposition, the electron cyclotron resonance CVD (ECRCVD) is a relatively promising technique that has been adopted to prepare a-$Si_{1-x}C_x$:H films due to its unique plasma properties such as high electron temperature and high ionization rate.[2] Another major advantage of the ECRCVD technique is that the energy of impinging ions on the films surface can be controlled independently from the degree of plasma ionization by applying a bias voltage to the substrates. This allows an extra degree of freedom in controlling the plasma properties and has been fully made use of previously in preparing various a-C:H films with properties ranging from polymericlike to diamondlike.[3]

Several works have been carried out on the effects of hydrogen dilution and reactant gas ratio on the properties of a-$Si_{1-x}C_x$:H films deposited by the ECRCVD process.[4,5] In contrast, the effects of bias voltage on such films have received relatively less attention. In general, dc or rf bias can

[a]Electronic mail: erusli@ntu.edu.sg

0021-8979/2001/89(11)/6153/6/$18.00 © 2001 American Institute of Physics

Downloaded 28 Jun 2001 to 137.132.3.5. Redistribution subject to AIP license or copyright, see http://ojps.aip.org/japo/japcr.jsp

TABLE I. The deposition conditions used and some properties of the a-$Si_{1-x}C_x$:H films deduced. The microwave power was set to 100 W and the gas flow ratio of SiH_4 (10% diluted in H_2):CH_4:H_2 was set to 20:2:100 sccm. The deposition pressure and substrate temperature were kept constant at 22 mT and 30 °C, respectively. E_{04} denotes the energy at which the absorption coefficient α is equal to 10^4 cm^{-1}, E_g and B are the Tauc band gap and the coefficient, respectively, extracted from the Tauc equation, E_0 is the Urbach energy and E_{pl} is the PL peak energy.

Sample	Bias (V)	C fraction	E_{04} (eV)	E_g (eV)	E_0 (meV)	B ($cm^{-1/2}$ $eV^{-1/2}$)	E_{pl} (eV)
SCJ21	−20	0.49	2.67	2.36	174.2± 8.2	751.2	2.11
SCJ22	−40	0.49	2.70	2.42	223.8± 8.7	687.4	2.13
SCJ23	−60	0.52	2.73	2.44	283.3±12.6	624.3	2.14
SCJ24	−80	0.54	2.96	2.63	329.3± 9.8	520.6	2.36
SCJ25	−100	0.55	3.02	2.67	358.1±10.7	438.7	2.40
SCJ26	−120	0.66	3.05	2.70	370.3±11.1	339.2	2.42

be applied to the substrate in an ECRCVD process, with the latter being most commonly used since it is less susceptible to charge built up on the growing film surface. In this work, a-$Si_{1-x}C_x$:H films deposited using the ECRCVD technique under different rf-bias voltages are investigated in terms of their optical and structural properties, using different characterization techniques such as Rutherford backscattering spectroscopy (RBS), transmittance/reflectance spectrophotometry, photothermal deflection spectroscopy (PDS), Fourier transform infrared (FTIR) absorption, Raman scattering, and room temperature photoluminescence (PL).

II. EXPERIMENT

The details and schematic diagram of the ECRCVD system used in this work can be found elsewhere.[2] All the films were deposited on two types of substrate simultaneously: (1) ⟨100⟩-oriented single-crystal Si wafers for film thickness, Raman scattering, IR absorption, and photoluminescence measurements and (2) Corning 7095 glass for optical transmittance and reflectance measurements, and also PDS measurement. All the substrates were cleaned in acetone and propanol, rinsed in deionized water, and dried in nitrogen ambient, before loading into the vacuum chamber. During the deposition, the gas flow ratio of SiH_4 (10% diluted in H_2):CH_4:H_2 was set to 20:2:100 sccm and the negative rf bias was varied from −20 to −120 V with the deposition pressure and substrate temperature kept constant at 22 mT and 30 °C, respectively. The microwave power was set to 100 W, which has been found to favor a-$Si_{1-x}C_x$:H films growth with lower defect density in our earlier study.[6] Table I summarizes the rf bias applied and some of the properties of the films deposited. The optical band gaps of the films were determined by transmittance and reflectance measurements using a dual beam Perkin–Elmer Lambda 16 spectrophotometer from 200 to 900 nm. The Tauc band gaps E_g and the B factor were extracted using the Tauc equation $(\alpha E)^{1/2}=B(E-E_g)$, where α is the absorption coefficient and E is the photon energy. The E_{04} gaps, defined as the energy at which α is equal to 10^4 cm^{-1}, were also determined for all the samples. The carbon fraction x ([C]/[C]+[Si]) in the a-$Si_{1-x}C_x$:H films was deduced using RBS. The RBS channeling has been done using 2 MeV He^+ to determine the content of C and Si on the (100) silicon substrate for samples SCJ21-24. The target normal was aligned with the beam in order to achieve a channeling geometry in which the signal from the Si substrate was reduced by an order of magnitude or so. A 50 mm^2 surface barrier detector mounted at 112° scattering angle was then used to collect the backscattering spectra. For samples SCJ25 and SCJ26, 2 MeV H^+ are used to determine the C and Si ratio as both samples are too thick for channeling. Here, the surface barrier detector is mounted at 20^0 scattering angle to detect the backscattered particles. PDS was used to measure the subgap absorption. The PDS spectra were measured from 250 to 650 nm and normalized to the absorption spectra deduced from UV–visible transmittance and reflectance measurements. The Urbach energy E_0 was extracted by fitting the exponential tail of the absorption coefficient curve to $\alpha=\alpha_0 \exp[(E-E^*)/E_0]$, where α_0 and E^* are constants. Infrared absorption measured using a FTIR spectrometer (Perkin–Elmer 2000) in the range of 400–3500 cm^{-1} was used to study the bonding in these a-$Si_{1-x}C_x$:H alloys. The Raman spectra were excited with a 244 nm line from a frequency doubled Ar^+ laser source and collected in a backscattering configuration by a charge coupled device camera using a Renishaw micro-Raman System 2000 spectrometer. PL measurements were carried out at room temperature using the 2.71 eV line from an Ar^+ ion laser source directed at near normal incidence to the sample. The PL spectra were detected in the reflection direction using a water-cooled Hamamatsu R2949 photomultiplier tube (PMT) based on single-photon counting technique through a 1/4 m double monochromator Digikrom DK242. The PL spectra were corrected for the combined response of the PMT and monochromator.

III. RESULTS AND DISCUSSION

Figure 1 shows the optical band gap E_{04} and E_g as a function of the rf bias applied to the substrate. The E_{04} is first seen to increase slowly from 2.67 to 2.73 eV when the bias changes from −20 to −60 V. When the bias is further increased to −80 V, the band gap exhibits a jump to 2.96 eV, beyond which it saturates gradually. The Tauc gap E_g also displays a similar variation with the bias voltage. The band gap behavior of a-$Si_{1-x}C_x$:H is more complex than those of a-Si:H and a-C:H due to alloying. A correlation between the band gap and carbon fraction x incorporated in a-$Si_{1-x}C_x$:H has been noted and was semiquantitively accounted for by Robertson[7] in terms of the different bonding types and their

Downloaded 28 Jun 2001 to 137.132.3.5. Redistribution subject to AIP license or copyright, see http://ojps.aip.org/japo/japcr.jsp

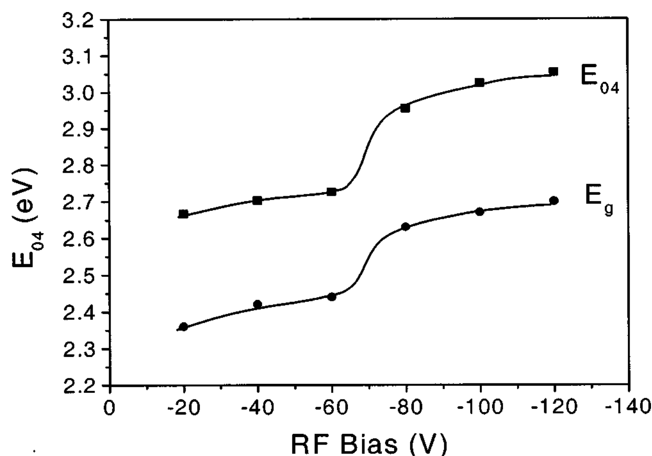

FIG. 1. Optical band gap E_{04} and E_g as a function of the bias voltage. The lines serve as a guide for the eye.

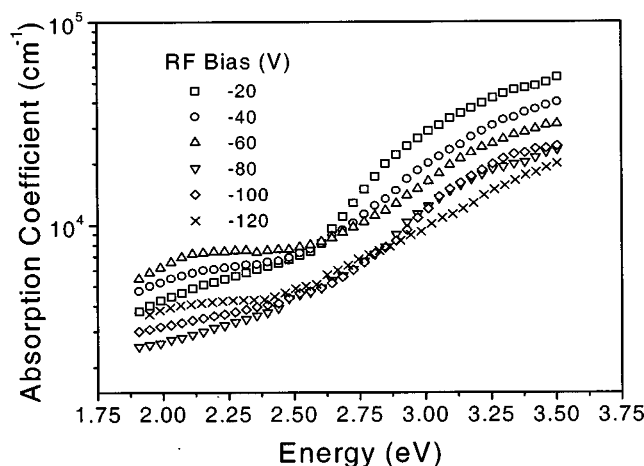

FIG. 2. Absorption coefficient spectra for all the films measured by PDS.

effects on the energy band structure. When x is increased to 0.5, the Tauc gap E_g opens up gradually mainly by lowering the valence band edge E_v as Si–Si bonds are replaced by stronger Si–C bonds. As x continues to increase to about 0.65, E_g opens up more rapidly as some Si–C bonds are replaced by the even stronger C–C bonds. For larger $x > 0.65$, the gap narrows in these C-rich alloys owing to the onset of substantial $C\,sp^2$ bonding.[7] Thus, in Si-rich a-$Si_{1-x}C_x$:H films, a monotonic relation exists between the carbon fraction x and band gap, which has been established and verified.[8] In this work, the carbon fraction x is 0.49 for the samples SCJ21 (−20 V) and SCJ22 (−40 V), and 0.52 and 0.54 for the samples SCJ23 (−60 V) and SCJ24 (−80 V), respectively (see Table I). Therefore, these four samples are near stoichimetric a-$Si_{1-x}C_x$:H films with the conduction and valence bands mainly controlled by Si–C bonds, and possibly also by C–C bonds for the latter two samples. As can be seen from Table I, x continues to increase gradually with the rf-bias voltage, with values of 0.55 and 0.66, respectively, for samples SCJ25 and SCJ26. These values of x are not expected to result in a decrease in the optical gaps, consistent with the results shown in Fig. 1. However, it should be cautioned that the effect of hydrogen incorporation should be considered as well in interpreting the relation between the fraction of carbon incorporated and the optical gap of the films. This can be illustrated by considering the samples SCJ23 and SCJ24 where a difference in the band gap is noted despite the fact that their carbon fractions are very similar, within the experimental error of the RBS measurement. The larger band gap of SCJ24 can be attributed to its higher hydrogen content, as can be seen from the IR absorption results (shown in Fig. 4), since hydrogenation is known to widen the gap in the tetrahedral Si–C band structure by lowering the valence band edge.[7]

The increase in carbon fraction at larger bias voltages can be understood by considering the predominant film surface chemistry. During deposition of the a-$Si_{1-x}C_x$:H films, carbon incorporation is generally much less efficient than silicon due to the high activation energy required for the electroimpact dissociation of CH_4 as well as for converting absorbed carbon species into bonded carbon in the solid film.[9] In the ECRCVD process, ion acceleration towards the substrate is usually caused by the sheath potential originating from the difference in the ion and electron velocities. An additional acceleration may be observed for ions confined in the divergent magnetic field. Electrons in the ECR plasma zone absorb microwave power and are accelerated to the region of lower magnetic field due to the interaction between their magnetic moments and the diverging magnetic field gradient. Through this electron drift an electrostatic drag is applied to the ions. The magnitude of this effect depends strongly on the magnetic field configuration as well as on the distance between the resonance zone and the substrate, and also the size of the substrate holder.[10] In our case of varying rf biasing under a constant microwave power and process pressure, the ECR plasma potential should not be significantly affected, and the ion energy will be mainly determined by the applied rf-bias voltage. Therefore, as the rf bias changes from −20 to −120 V, the larger substrate potential will increase the energy of the impinging carbon species, resulting in an increase in the carbon fraction in the films. Besides, this will also render the conversion of absorded carbon species into bonded carbon much more efficiently.

Figure 2 shows the absorption coefficient spectra for all the films measured by PDS. It can be seen that the optical absorption in the films at higher energy are weakened and the absorption coefficient spectra are flattened when the bias voltage is increased. This suggests increasing Urbach tail width and also widening of the optical band gap. A similar result has been observed by Fathallah,[11] and is generally attributed to a large potential fluctuation caused by the incorporation of carbon atoms into the a-Si:H network. These results therefore suggest that the structural disorder in the a-$Si_{1-x}C_x$:H films scales with the rf-bias voltage monotonically. The detailed variation of the Urbach energy E_0 with the bias voltage is shown in Fig. 3. The absorption near the band tail for some of the samples do not exactly follow the exponential trend (see Fig. 2) but instead reveal some structures that could be caused by subgap states in the films. In this case, E_0 is deduced by obtaining the best exponential fit for the absorption tail and the uncertainty involved are

Downloaded 28 Jun 2001 to 137.132.3.5. Redistribution subject to AIP license or copyright, see http://ojps.aip.org/japo/japcr.jsp

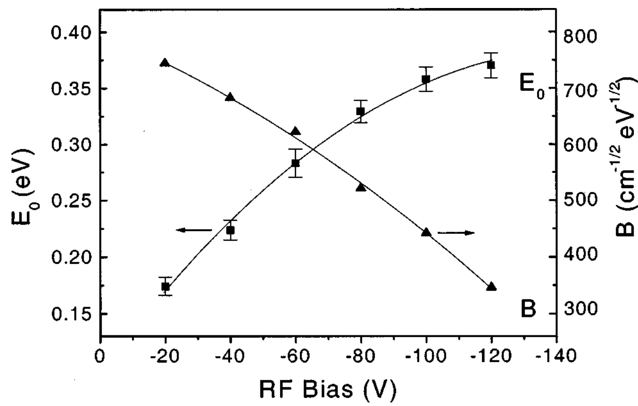

FIG. 3. Urbach energy E_0 and B factor measured by PDS and transmittance/reflectance spectrophotometry as a function of the bias voltage. The lines serve as a guide for the eye.

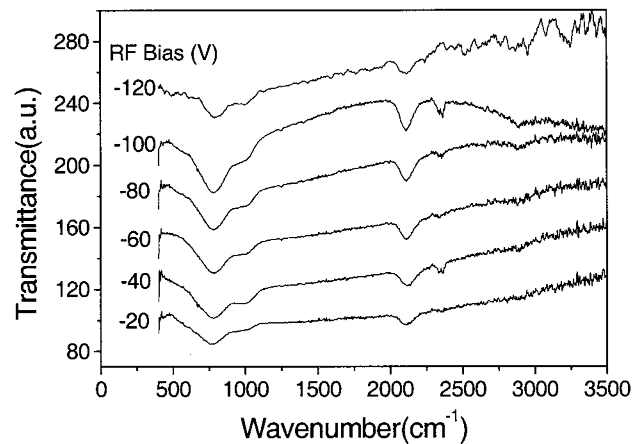

FIG. 4. Fourier transform IR transmittance spectra for all the films deposited at different bias voltages and corrected for their thickness.

shown in Fig. 3. It can be seen that E_0 increases rapidly over the rf-bias range from -20 to -60 V and more gradually from -80 to -120 V. The relation between E_0 and carbon fraction x in the a-$Si_{1-x}C_x$:H films seen in this work is similar to that reported previously,[12] which found that E_0 scaled with carbon fraction x dramatically for $x<0.6$ and then more gradually for $x>0.6$. Besides the Urbach slope E_0, the Tauc slope B factor as measured by PDS and transmittance/reflectance spectrophotometry is also shown in Fig. 3 to further study the degree of disorder in the films. The B factor has also been previously taken as a measure of the structural disorder in a-$Si_{1-x}C_x$:H films, with a higher value of B indicating a smaller degree of structural disorder.[13] It should be noted that the exact correlation between E_0 and B factor with the structural disorder in a-$Si_{1-x}C_x$:H is still unclear at present. Although it is generally agreed that E_0 is related to local structural disorder (microstructural disorder due to alloying) and B is related to overall structural disorder,[13] some previous studies[5,7] have found that microstructural disorder resulted in an increasing overall disorder, whereas other work[14] noted that the overall disorder remained nearly unchanged. The B factor in this work is seen to decrease with increasing bias voltage, and a linear correlation between E_0 and B factor can be established

$$E_0(\text{meV}) = 559 - 0.48B(\text{cm}^{-1/2}\ \text{eV}^{-1/2}).$$

The result suggests that the local defects related to microstructural disorder resulting from alloying with carbon dominate the overall defect structure of the films.

Figure 4 shows the Fourier transform infrared transmittance spectra for the films, corrected for their thickness. The predominant peak at 780 cm^{-1} seen in all the films can be attributed to the Si–C stretching mode or Si–CH_3 wagging mode. Katayama *et al.*[15] noted that this mode has similar strength in sputtered alloys prepared with and without hydrogen, and therefore we assign it to the Si–C stretching mode for our films. The shoulder peak located around 1000 cm^{-1} corresponds to the C–H_n wagging mode to which silicon atoms are attached. Another obvious peak for all the films occurs at around 2100 cm^{-1}, which corresponds to Si–H_n stretching modes. The C–H_n stretching mode at 2900 cm^{-1} is very weak for the samples SCJ21–SCJ23, but gradually increases in strength for the samples SCJ24–SCJ26. This suggests increased carbon and hydrogen fractions in these samples, contributed by the larger amount of hydrocarbon species incorporated at higher bias voltages. As argued earlier, this enhanced hydrogenation can account for the difference in the optical gap between the samples SCJ23 and SCJ24, despite their similar carbon fraction. The increase in the hydrogen and carbon fractions can also be seen from the stronger Si–C (790 cm^{-1}) and Si–H_n (2100 cm^{-1}) absorption when the bias voltage is increased from -20 to -100 V. For the sample SCJ26 (-120 V), due to its larger carbon fraction, the C–H_n bonds at around 1000 and 2900 cm^{-1} are strengthened while the silicon related bonds at 790 and 2100 cm^{-1} are relatively weakened. The increased carbon incorporation can result in the formation of carbon sp^2 clusters, as will be shown from the Raman scattering results shortly. However, the present results suggest that these clusters are not sufficiently large to result in a lowering of the band gap of the films.

Figure 5 shows the Raman spectra for all the films deposited under different bias voltages. The Si–Si bond ex-

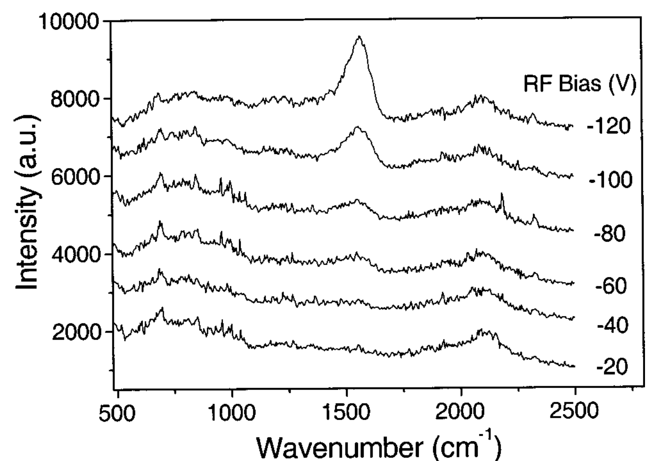

FIG. 5. Raman spectra for all the films deposited under different bias voltages.

Downloaded 28 Jun 2001 to 137.132.3.5. Redistribution subject to AIP license or copyright, see http://ojps.aip.org/japo/japcr.jsp

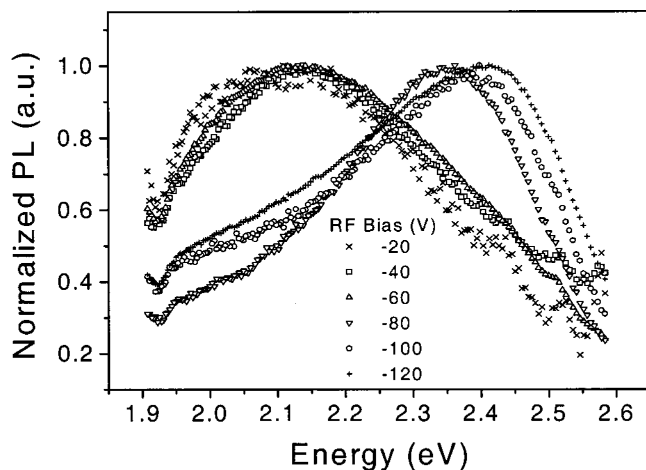

FIG. 6. Normalized room temperature PL spectra for all the samples deposited under different bias voltages. Excitation energy $E_{ex}=2.71$ eV.

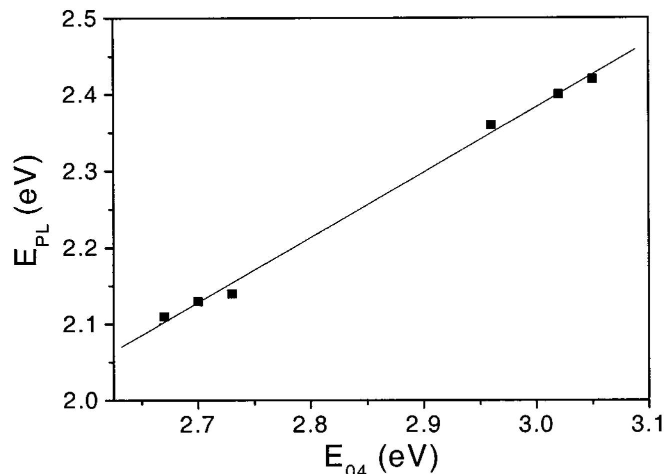

FIG. 7. Variation of E_{pl} with the E_{04} gap.

pected around 480 cm^{-1} (that range not shown in the figure) is not obvious in all the spectra. However, a wide band from 600 to 1000 cm^{-1} corresponding to Si–C bonds can be clearly seen for all the samples. It is noteworthy to mention that since the Raman scattering efficiency of Si–C bond is much lower than that of C–C bond, previous study[16] has failed to detect this band in their Raman spectra, even for some Si-rich a-$Si_{1-x}C_x$:H samples.[17] Therefore, the obvious Si–C bonds observed in Fig. 5 implies that all the films consist of a substantial amount of Si–C bonds. A broad band around 2093 cm^{-1} corresponding to Si–H_n bond can also be seen for all the samples, which is in good agreement with the earlier FTIR results. A peak at 1565 cm^{-1} corresponding to optical-like modes of highly disordered graphitic carbon (C═C), which increases in strength with the bias voltage, is observed for the samples SCJ24–SCJ26. This C═C bond strength variation, coupled with the obvious Si–C band observed for all the films, suggests larger carbon fractions for samples grown at larger bias voltages, consistent with the results shown in Table I. Our earlier study[6] on a-$Si_{1-x}C_x$:H deposition at varying microwave power and under no bias condition did not reveal any obvious Si–C bond in the Raman spectra. The Raman results shown in this work therefore indicate that substrate biasing is crucial to the formation of Si–C bonds in the films. From the Raman scattering results, it is also suggested that the films deposited at lower bias voltages (−20, −40, and −60 V) possess relatively higher chemical order compared to those deposited at larger bias voltages, due to the absence of C═C bonds. This is consistent with the results shown in Fig. 3.

Figure 6 shows the normalized room temperature PL spectra for all the samples deposited under different bias voltages and Fig. 7 shows the variation of the PL peak energy (E_{pl}) with the band gap E_{04}. The E_{pl} ranges from 2.11 to 2.42 eV and exhibits an almost linear relation with the E_{04} gap whereas the full width at half maximum (FWHM) of the PL band remains relatively constant at around 0.5±0.05 eV for all the samples. Although Conde *et al.*[5] have observed that the E_{pl} did not vary with the optical band gap E_{04} for a-$Si_{1-x}C_x$:H films deposited by the ECRCVD process, the linear relation between E_{pl} and E_{04} has been observed in several studies[18,19] and is a general feature of PL in several amorphous semiconductors such as a-Si:H, a-C:H, and a-$Si_{1-x}C_x$:H, attributed to tail-to-tail states recombination. This is also observed in our samples despite that the excitation energy used $E_{ex}=2.71$ eV is below the E_{04} gap of the samples, except for the two deposited at −20 and −40 V. Under subgap excitation at a given E_{ex}, the states that are participating in radiative recombination are deeper down into the band tails for films with larger band gap, which therefore leads to less thermalization steps involved for the carriers and hence a larger E_{pl}. Under the tail-to-tail states PL recombination model, the FWHM of the PL is generally expected to increase with the Urbach tail width. However, this is not observed in our samples. This is because for $E_{ex} < E_{04}$, despite the larger Urbach energy E_0 that would lead to a wider FWHM for samples deposited at larger bias voltages, the higher optical gap would result in deeper subgap excitation and hence a narrower FWHM. Therefore, overall the FWHM may not be affected much, as can be seen from the nearly constant FWHM across all the samples.

Figure 8 shows the relative quantum efficiency (RQE) of the PL as a function of the band gap E_{04}. The RQE is the integrated PL intensity corrected for the absorption, thickness, and reflection coefficient of the films. It can be seen that for samples SCJ21–SCJ23 the RQE is relatively constant, and for samples SCJ24–SCJ26 the RQE increases roughly exponentially with the band gap. For a carbon fraction of less than 0.5, the structure of Si-rich a-$Si_{1-x}C_x$:H is expected to consist of a tetrahedrally coordinated amorphous network of Si–Si bonds, with the C atoms incorporated in a terminating or bridging configuration. In this case, the PL mechanism is expected to be similar to that observed in a-Si:H, with long radiative lifetimes and a strong temperature dependence, and in which tunnelings between localized states are involved. The Si dangling bonds acting as nonradiative recombination centers form the main recombination channel which causes the PL efficiency to decrease rapidly with increasing temperature and defect density. The PL efficiency η varies with the paramagnetic spin density N_s as

Downloaded 28 Jun 2001 to 137.132.3.5. Redistribution subject to AIP license or copyright, see http://ojps.aip.org/japo/japcr.jsp

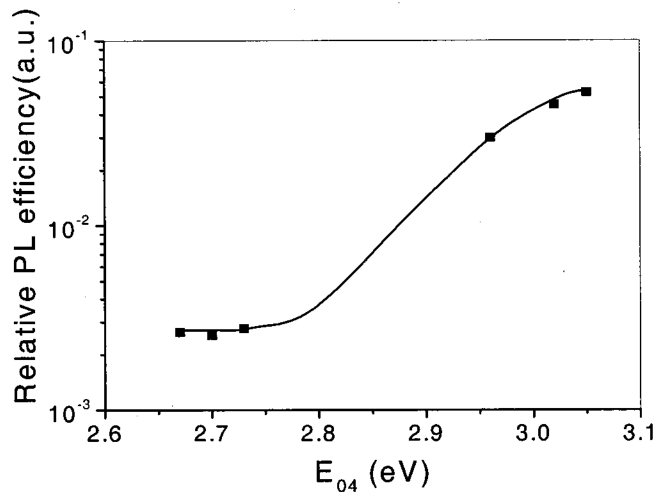

FIG. 8. RQE of the PL as a function of the E_{04} gap.

$$\eta = \eta_0 \exp(-\tfrac{4}{3}\pi R_c^3 N_s),$$

where R_c is the capture radius of the defects. Room temperature visible PL can be observed from samples SCJ21–SCJ23 (with bias voltages -20, -40, and -60 V, respectively) despite their relatively lower PL RQE. This suggests that the electronic band structures of these samples are controlled by Si–C bonds instead of Si–Si bonds, as can also be seen from the Raman scattering results. This, coupled with the fact that $x \approx 0.5$ for these samples, suggests that silicon dangling bonds which generally quench the PL are not expected to be significant in these films. For samples SCJ24–SCJ26 which contain significant C–C bonding as deduced from the Raman spectra, the PL can be attributed to emission resulting from monomolecular radiative recombination of the photogenerated electrons and holes, which could be localized in the sp^2 clusters. In this case, the PL shows short lifetime, weak temperature dependence, and relatively high efficiency, and is not quenched by applied electric field.[5] In C-rich a-$Si_{1-x}C_x$:H, Liedtke *et al.*[20] found little correlation between PL efficiency and spin density, suggesting that the recombination is not particularly associated with defects. For samples SCJ24–SCJ26, the variation of nearly exponentially increasing RQE versus E_{04} has also been observed in the PL study of pure a-C:H reported by Rusli *et al.*[21] Finally, note that Conde *et al.*[5] could not observe room temperature PL from their ECRCVD deposited Si-rich a-$Si_{1-x}C_x$:H films. The observation of room temperature PL from the samples SCJ21 to SCJ23 in this work suggests that using a low microwave power of 100 W and a low negative rf-bias voltage (less than -60 V) in an ECRCVD process can result in lower defect density and near stoichimetric a-$Si_{1-x}C_x$:H films.

IV. CONCLUSION

Hydrogenated amorphous silicon carbide (a-$Si_{1-x}C_x$:H) films have been deposited using the ECRCVD process by varying the rf-bias voltage at the substrate. The effects on the optoelectronic and structural properties of these films are investigated. It is found that the rf-bias voltage can influence the carbon fraction x incorporated in the a-$Si_{1-x}C_x$:H films. When the rf-bias voltage is increased from -20 to -60 V, near stoichimetric a-$Si_{1-x}C_x$:H films ($x \approx 0.5$) can be achieved with gradually increasing carbon fraction and optical band gap. For these films, the electronic bands are mainly controlled by the Si–C bonds. There is also an increase in the hydrogen content at larger bias voltages, as verified by the FTIR results. For these samples, visible room temperature PL with relatively low efficiency can be observed and the number of Si dangling bonds is expected to be small. When the rf-bias voltage is further increased from -80 to -120 V, the carbon fraction increases, resulting in slightly C-rich a-$Si_{1-x}C_x$:H films ($x > 0.5$) with larger optical band gap. For these films, carbon sp^2 clusters formation is observed, which enhances with increasing bias voltage as deduced from the Raman spectra. The PL of these samples are similar to that of C-rich a-$Si_{1-x}C_x$:H featured by the relatively higher PL efficiency. For all the films, the disorders have been shown to increase with increasing rf-bias voltage monotonically. The linear relationship observed between the Urbach tail width E_0 and the B factor in the Tauc equation suggests that the local defects related to microstructural disorder resulting from alloying with carbon dominate the overall defect structure of the films.

[1] Y. Hamakawa, T. Toyama, and H. Okamoto, J. Non-Cryst. Solids **115**, 180 (1989).
[2] S. F. Yoon, R. Ji, J. Ahn, and W. I. Milne, Diamond Relat. Mater. **5**, 1371 (1996).
[3] Rusli, S. F. Yoon, H. Yang, J. Ahn, Q. Zhang, and W. L. New, J. Appl. Phys. **84**, 5277 (1998).
[4] Y. Hamakawa and H. Okamoto, Mater. Res. Soc. Symp. Proc. **242**, 651 (1992).
[5] J. P. Conde *et al.*, J. Appl. Phys. **85**, 3327 (1999).
[6] J. Cui, Rusli, S. F. Yoon, M. B. Yu, K. Chew, J. Ahn, Q. Zhang, E. J. Teo, T. Osipowicz, and F. Watt, J. Appl. Phys. **89**, 2699 (2001).
[7] J. Roberston, Philos. Mag. B **66**, 615 (1992).
[8] D. Della Sala, P. Fiorini, A. Frova, A. Gregori, A. Skumanich, and N. M. Amer, J. Non-Cryst. Solids **77–78**, 853 (1985).
[9] S. T. Ceyer, Science **249**, 133 (1990).
[10] P. Reinke, W. Jacob, and W. Moller, *Diamond and Diamond-like Films and Coatings* (NATO-ASI, Castelveccio, Italy, 1989).
[11] M. Fathallah, J. Non-Cryst. Solids **164–166**, 909 (1993).
[12] F. Boulitrop, J. Bullot, M. Gauther, M. Schmit, and Y. Catherine, Solid State Commun. **54**, 107 (1985).
[13] R. Tsu, P. Menna, and A. H. Mahan, Sol. Cells **21**, 189 (1987).
[14] Y. Tawada, K. Tsuge, M. Kondo, H. Okamoto, and Y. Hamakawa, J. Appl. Phys. **53**, 5273 (1982).
[15] Y. Katayama, D. Kruangam, and T. Shimada, Philos. Mag. B **43**, 283 (1981).
[16] F. Demichelis, C. F. Pirri, and E. Tresso, J. Appl. Phys. **72**, 1327 (1992).
[17] W. K. Choi, F. L. Loo, C. H. Ling, F. C. Loh, and K. L. Tan, J. Appl. Phys. **78**, 7289 (1995).
[18] D. Kruangam, T. Endo, G. P. Wei, S. Nonomura, H. Okamoto, and Y. Hamakawa, J. Non-Cryst. Solids **77–78**, 1429 (1985).
[19] V. Chu, J. P. Conde, J. Jarego, P. Brogueira, J. Rodriguez, N. Barradas, and J. C. Soares, J. Appl. Phys. **78**, 3164 (1995).
[20] S. Liedtke, K. Jahn, F. Finger, and W. Fuhs, J. Non-Cryst. Solids **97**, 1083 (1987).
[21] Rusli, J. Robertson, and G. A. J. Amaratunga, J. Appl. Phys. **80**, 2998 (1996).

Downloaded 28 Jun 2001 to 137.132.3.5. Redistribution subject to AIP license or copyright, see http://ojps.aip.org/japo/japcr.jsp